

#### **4. FIELD EMISSION FROM MANUFACTURED CARBON NANOTUBE ELECTRON SOURCES**

Research has been carried out into field emission properties of CNTs as electron sources as described in chapter 1. However, this was on CNTs attached to tungsten tips rather than grown directly upon them. Emission from CNTs grown by the arc discharge method, which produces CNTs inherently more crystalline than those produced by PECVD, has also been investigated. There has also been a tendency to show the best results, rather than typical results. CNTs that produce the smallest spot size will not necessarily have the smallest kinetic energy spread, nor be the most stable.

It is, in fact, very difficult to determine the optimum geometry for CNT electron sources. The best geometry for stability will be different from the best geometry for kinetic energy spread, which in turn will be different from that for best reduced brightness. It will not necessarily be the same from that which produces the smallest virtual source size. To pick an example, a small virtual source size means that electrons will originate from a very small area of the CNT. The electrons within the beam are therefore more likely to repel each other (the Boersch effect) and produce a larger spot size than could be achieved with a larger source size. A small virtual source will almost certainly result in a higher kinetic energy spread also. Stability depends on the nature of the particle that attaches to the tip and the tip geometry and will be discussed later in this chapter.

This chapter will compare the field emission properties of CNTs with measurements made elsewhere. It will outline the problems with CNT sources that are not detailed in publications thus far, some of which have been overcome during the work. Exaggeration serves no purpose: issues with CNT sources are not insurmountable, they just need to be addressed. If CNT sources are ever going to be available on the market, a proper comparison should be made with sources already available and this chapter aims to do this. No ballast resistor was used whilst taking this data. As will be discussed in chapter 5, the introduction of a ballast resistor increases current stability.

## 4.1 MOUNTING OF CNTS FOR DATA COLLECTION

Three different approaches were taken to collect the data. The first was to use the CNTs grown on individual tungsten wires; the second, to use CNTs grown on the wire attached to a Philips heating filament; the third, to use CNTs grown on tungsten whilst mounted in an electron source module. These three methods are described in more detail below.

### 4.1.1 ELECTRON SOURCES GROWN ON SINGLE TUNGSTEN WIRE PIECES

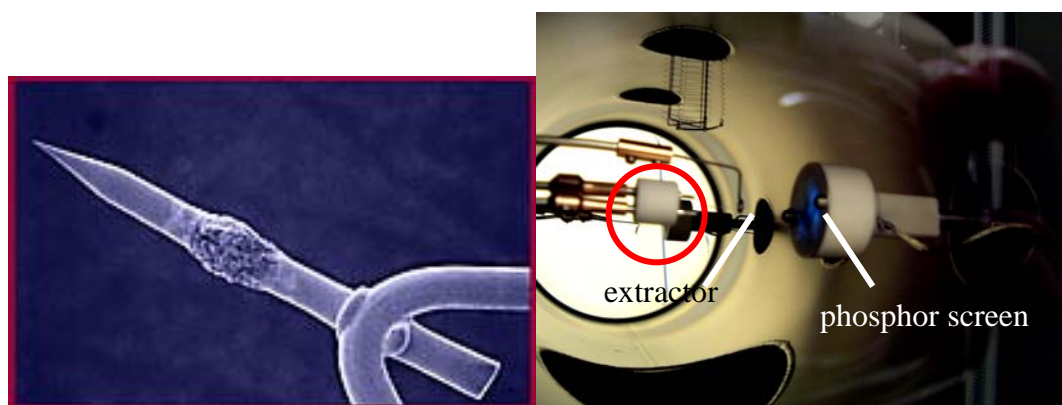


Figure 4.1.1: Left, shows a picture of a tungsten tip spot-welded to a standard FEI Schottky base. The tip is heated by passing current through the filament which conducts to the tip. Right, shows the tip in a vacuum system during field emission measurements. The red circle denotes the position of the Schottky base. The current is extracted by the extractor which consists of a small metal loop situated  $500\ \mu\text{m}$  from the tip apex. The total current can simply be calculated from the extraction voltage and the power. Electrons in the beam scintillate a phosphor screen showing the emission pattern. Bright spots indicate points of high intensity. A Faraday cup is located in the centre of the phosphor screen. From this, the angular current density can be calculated.

The first field emission data came from CNTs grown directly onto etched tungsten wire. The wire was taken to the FEI Company, Oregon, USA and welded to a Schottky base as shown in figure 4.1.1. The tips were then mounted in a vacuum

system designed to test new field emission sources. The tips were heated by passing current through the filament that the tungsten wire was welded to and an extractor placed 500  $\mu\text{m}$  above the apex of the wire to extract the current. The emission pattern was observed using a phosphor screen which was positioned approximately 4 cm from the extractor. In the centre of the phosphor screen, a Faraday cup 40  $\mu\text{m}$  in diameter was used to calculate the angular density of the electron beam. Data were recorded by software at various intervals which were determined by the measurements being taken.

Tips mounted in this way will be referred to as FEI tips in the rest of this chapter.

#### **4.1.2 MOUNTING OF ELECTRON SOURCES WITH A PHILIPS HEATING FILAMENT**

The Philips sources were placed in a specially designed clamp which was also used to pass current through the heating filament. The two feet were separated by an insulating ceramic spacer. Firstly, the clamp was fed into a roughing chamber, as the main chamber is constantly maintained at high vacuum. Upon reaching low pressure, the tip was fed into the main chamber by a system of levers (see figure 4.1.2).

The system consists of many devices that can be used to measure the various field emission properties of the tip. This system was used primarily for emission pattern, stability and energy spread measurements. Tips mounted in this way will be referred to as Philips tips in the remainder of this chapter.

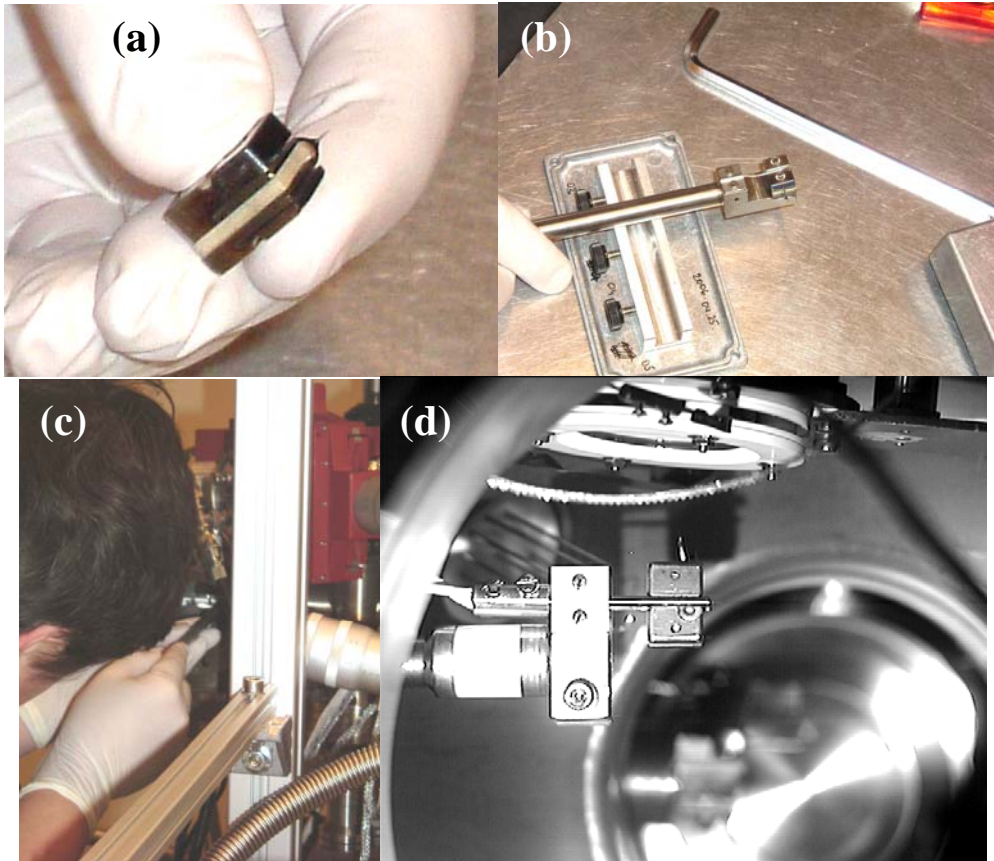


Figure 4.1.2: Mounting of the Philips source into the field emission chamber. (a) shows the holder. Current is fed through the thick, U-shaped filament through the clamp used to hold it. The two feet are insulated by a ceramic spacer. It is mounted onto a holder (b) to be fed into a pumping chamber (c). It is then fed by a system of levers into the centre of the main chamber which is constantly maintained at high vacuum for various field emission measurements, as shown in (d).

### 4.1.3 ELECTRON SOURCES MOUNTED IN ELECTRON GUNS

In this process, the entire suppressor/Schottky module is placed into a growth chamber. Whilst there is only one CNT grown at the apex of the tungsten tip, the suppressor is also coated in CNTs (as in figure 4.1.3).

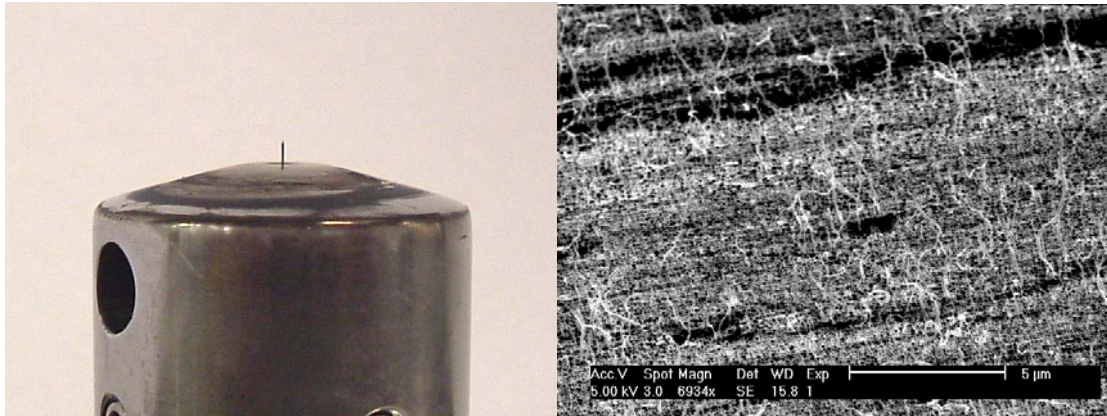


Figure 4.1.3: Covering of suppressor with CNTs. Note *left* how the suppressor is black on top. This is due to a mixture of CNTs and amorphous carbon, both of which have a black appearance. The CNTs grown on the suppressor can clearly be seen *right*.

The dirty suppressor is removed and replaced with a clean one because the tips are pre-aligned, so all parts are interchangeable. The old suppressor can be recycled and used for further CNT growth. The new suppressor and tip are placed inside an electron gun module which is then placed inside a field emission chamber for testing. Tips mounted in this setup will be referred to as York tips in the rest of this chapter.

#### 4.1.4 FIELD EMISSION CONFIGURATION SUMMARY

Below in table 4.1.4 is listed a summary of the characteristics of the various field emission configurations described above.

Table 4.1.4: Configuration summary.

Configuration	Geometry	Extractor-tip separation
FEI tips	Etched, pre-grown tips welded to Schottky base	500 $\mu\text{m}$
Philips tips	Etched, pre-grown tips welded to U-shaped heating filament	4 cm
York tips	Etched tips, post-grown in pre-aligned suppressor module	500 $\mu\text{m}$ with suppressor 70 $\mu\text{m}$ below tip

## 4.2 FIELD EMISSION DATA

The field emission data for CNTs grown onto tungsten tips and mounted by the three different methods are collated here. Firstly, how to switch the CNT on will be described. Later, the stability, energy spread, brightness and virtual source size will be detailed and compared to other sources. The CNTs used to collect the data are inset within the figures and their dimensions are described in detail in Appendix A.

### 4.2.1 COMPLETING THE CAP STRUCTURE

Minoux et al. [1] reported the structural changes of CNTs under rapid thermal annealing. As described in chapter 3, at the moment deposition finishes in PECVD, CNTs do not have a graphitic covering around the top of the catalyst particle.

They instead are covered in amorphous carbon, which is converted into graphene walls when heated to 1100 °C for 6 minutes. The same process was repeated here. After the CNT tips were loaded into the chamber, pumped and baked until the pressure reached  $10^{-10}$  mBar, a pyrometer was focused on the apex of the tip and the tip heated to 1100 °C for 6 minutes. This affects the tip in two ways. It alters the emission pattern and increases the stability of the field emission coming from the tip. Figure 4.2.1.1 shows field emission from an FEI tip immediately before and after heating. Note that the emission current is quite noisy in figure 4.2.1.1a, but after heating the current is more stable, shown in figure 4.2.1.1b. Note that the current still shows significant variation after annealing. This will be explained in the next section.

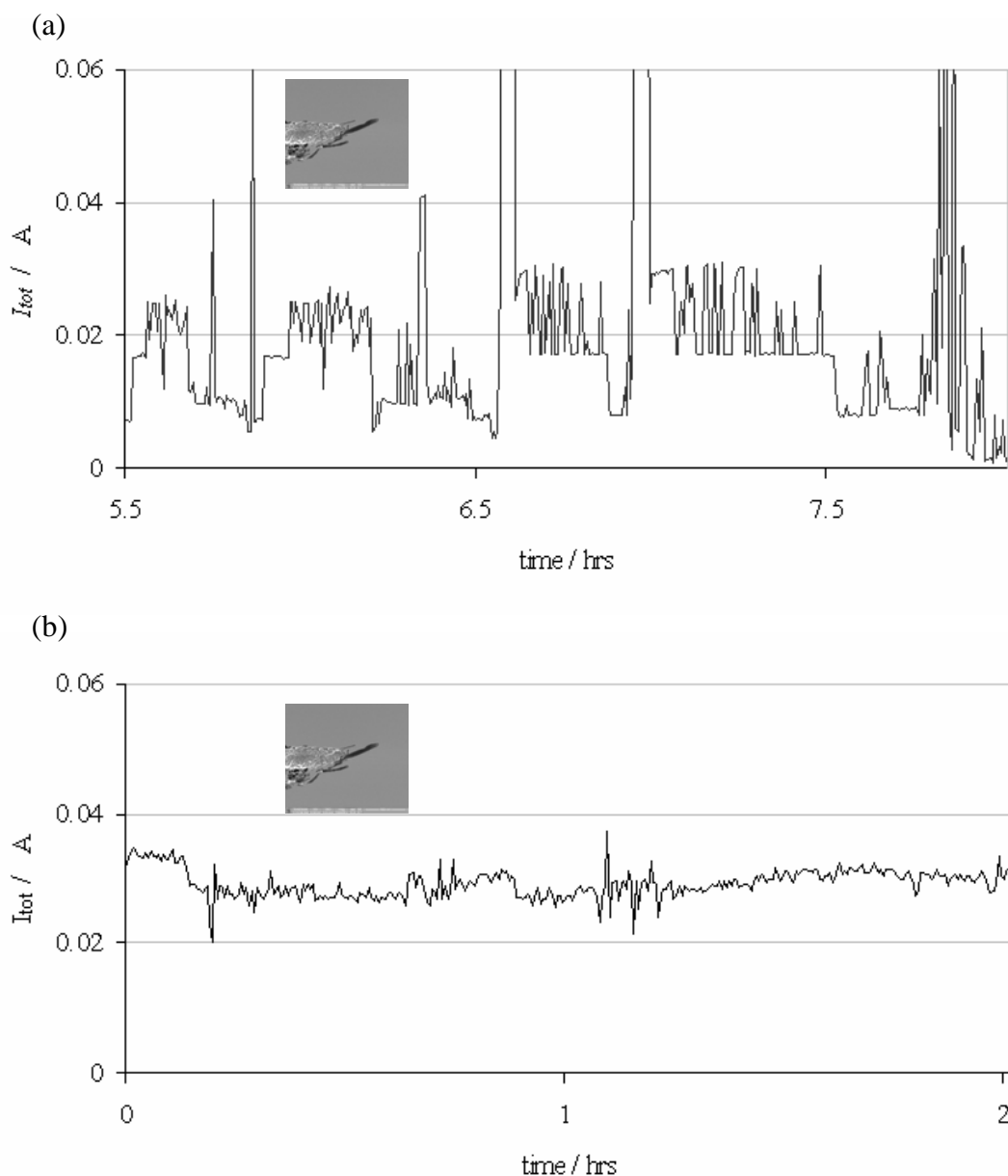


Figure 4.2.1.1: (a) shows field emission from a CNT before thermal annealing. The total current,  $I_{tot}$ , is plotted on the y axis, against the time in hours on the x axis. The current can be seen jumping around erratically. (b) shows the same tip after thermal annealing at 1100 °C for 6 minutes with the same variable on both axes. The current is more stable with a lot less variation in the current. The inset shows a small image of the CNT source used.

Figure 4.2.1.2 shows a sequence of field emission patterns for a Philips tip. Various sites are observed to switch on and off which indicates continual changing in the

structure of the tip, with molecules adsorbing and desorbing. No stable field emission is observed.

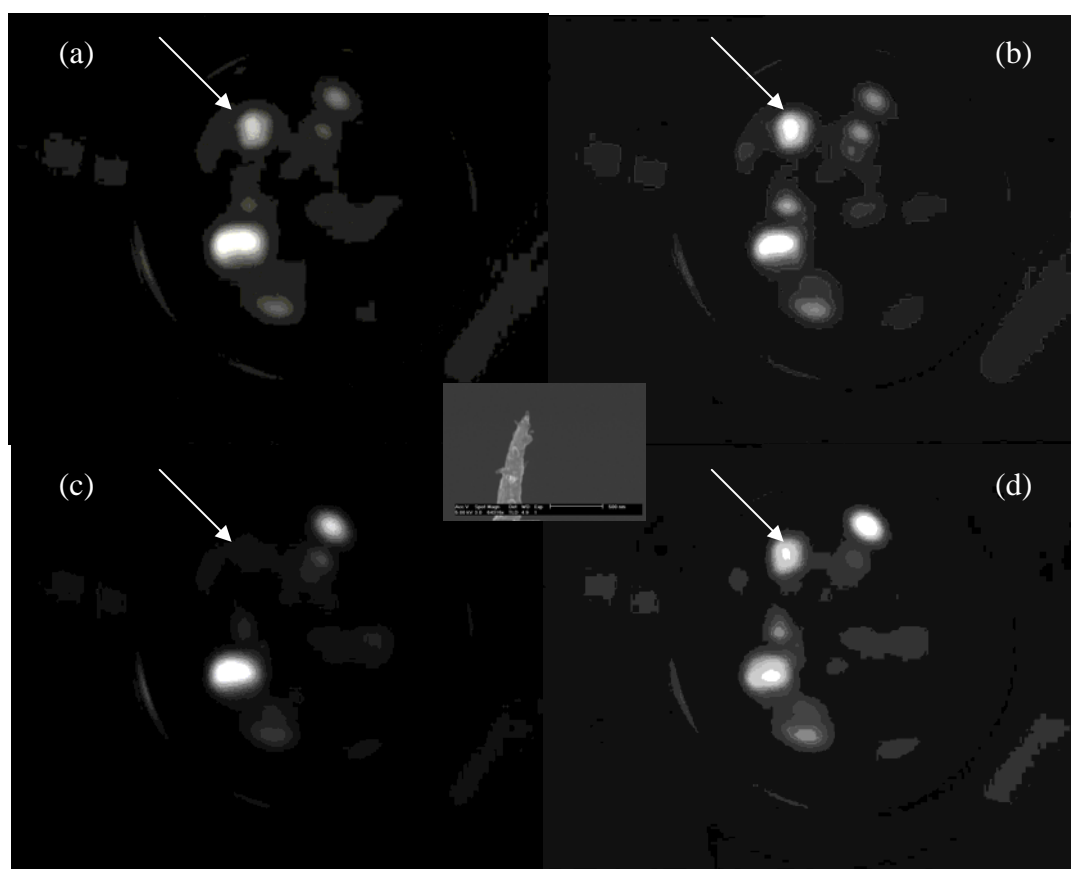


Figure 4.2.1.2: A sequence of images in chronological order taken a few minutes apart showing the field emission pattern from a Philips CNT, inset, before the annealing step. Note how the dots highlighted with the white arrow switch on and switch off. High instability is observed in the field emission pattern. Note how the relative intensity of the bright areas also varies.

There is also a lack of an overall pattern in figure 4.2.1.2. The bright areas seem to be randomly distributed and do not exhibit the characteristics of field emission from a surface with a crystalline structure. Figure 4.2.1.3 shows the same tip after the annealing process has been carried out. Note how the field emission pattern has four bright spots (a fifth was observed but it was not possible to fit the entire emission pattern onto the phosphor screen) and they appear to change little throughout the sequence of images.

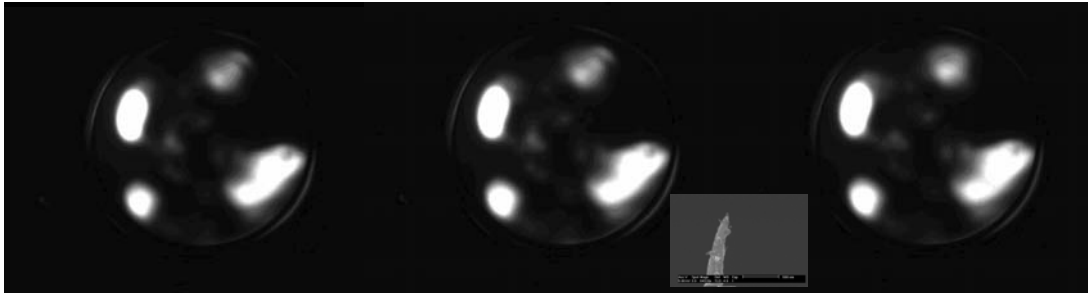


Figure 4.2.1.3: A sequence of images taken a few minutes apart showing the field emission pattern from a Philips CNT, inset, after the annealing step. Four bright areas can be seen. A fifth was located just off the bottom of the screen completing a pentagonal structure. There is little variation between the images.

#### 4.2.2 THE FIRST FEW HOURS OF EMISSION FROM CNTS

During the fabrication process, the tungsten wire is situated in a chamber with a variety of gases at a pressure one billion times that typically used to operate electron sources. The plasma breaks the gases up and when the CNTs form, hydrogen is given off. This results in both the tip and CNT absorbing and adsorbing many gaseous species, including the reactant gases, reduced gases and hydrogen. Consequently, during the first few days of emission, the measured current is quite variable as the adsorbed gas desorbs into vacuum. Figure 4.2.2.1 shows the first week of field emission data taken for two FEI tips.

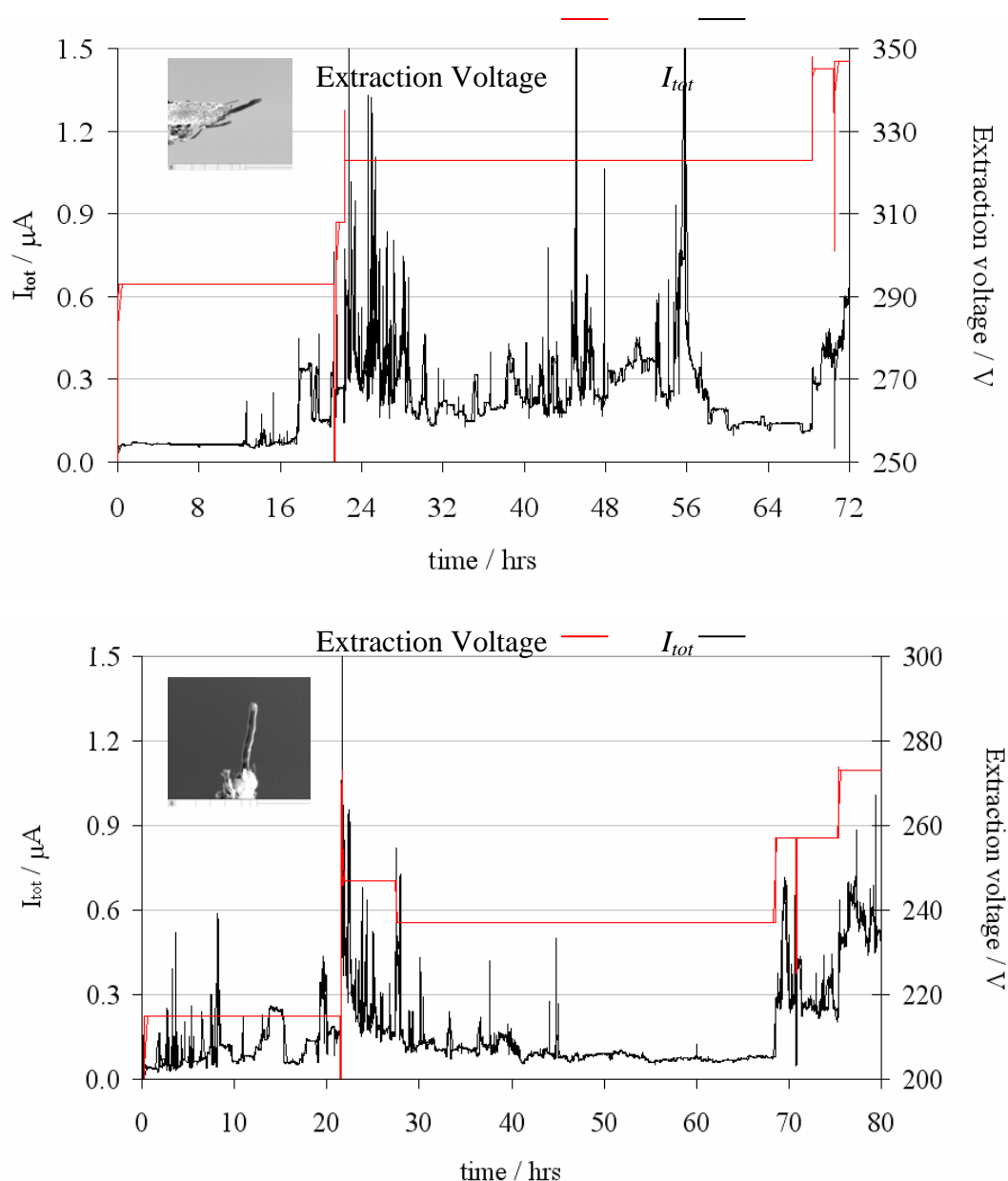


Figure 4.2.2.1: The first week of field emission data taken from two FEI tips (images inset). The total current,  $I_{tot}$ , (in black) and the extraction voltage (in red) are plotted against time. Note the instability of the electron source for fixed voltage over the first 50-60 hours of emission. At this point the total current reduces and becomes increasingly stable. It is only after this length of time that the field emission is stable enough to collect the various data required and thus is good enough to be considered as a source in an electron microscope.

To optimize CNT field emission performance, particularly to improve current stability, conditioning of the tip needs to occur. This was carried out by an initial rapid thermal anneal (described above) and by regular subsequent flashing. After rapid thermal

annealing, where the CNTs were rapidly heated to 1100 °C for 6 minutes at an initial pressure of  $1 \times 10^{-9}$  mbar, the tips were maintained at a temperature of 500 °C throughout field emission measurements to increase stability (as performed by De Jonge et al [2]). Rapid thermal annealing is distinct from flashing, which is a more general term for the heating of the tip by either heating or with the use of high ( $>1$   $\mu\text{A}$ ) total currents. Flashing by heat involved a process similar to rapid thermal annealing. Flashing with self-heating by high current is typically a more drawn out process, where the current is held at a few  $\mu\text{As}$  for up to an hour.

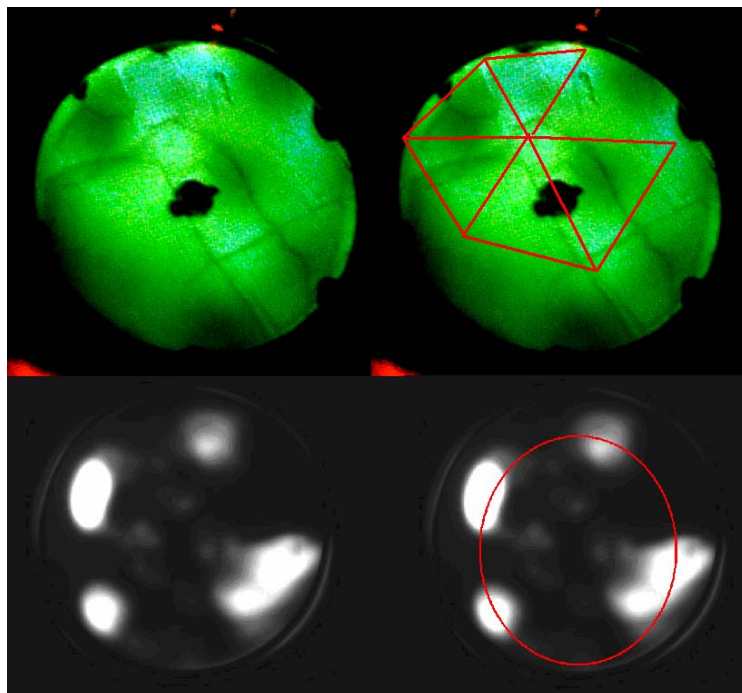


Figure 4.2.2.2: Field emission patterns of Philips electron sources. The top two images show a typical emission pattern from polycrystalline tungsten where the CNT has been removed. The right hand image shows the same pattern with red lines that indicate the structure and symmetry of the pattern. Note how there is little contrast between central bright spots and bright spots at the edge and how intensity is quite uniform across the phosphor screen. The bottom two images show the emission pattern of a CNT in the same system with the same geometry. The pattern is more compact, with huge contrast between the bright spots. The right-hand picture has a red line to show that the pattern has a circular geometry. Combined with the extraction voltage, it is easy to see at what point the CNT fails.

Note that the CNTs' respective turn-on voltages differ (293 V and 215 V: a difference of 78 V, or 30% difference). This is down to two factors: the inconsistency in the extractor-tip distance and the different dimensions of the CNTs. Indeed, there was a wide range of turn-on voltages for the many CNTs used for field emission data in this set-up. The turn-on point has been defined as the point at which there is 1 nA in total current, which is sufficiently high to be able distinguish from background noise. These were 278 V, 309 V, 375 V, 377 V, 280 V and 311 V.

Some tips were found to turn on at higher voltages than this, but this was found to be because the tip had lost its CNT. It was not discovered until a third of the way through the data collection that the tips were susceptible to electrostatic discharge. Consequently, some tips switched on at 600 V and above, which for the geometry was too high and was more likely to be caused by the tungsten itself field emitting. One other way of telling the difference between CNT field emission and tungsten emission is the difference in the appearance of the field emission patterns. A typical pattern for CNT field emission is a few bright spots circularly symmetrical about the centre. The pattern also seems to be quite compact. By contrast, the tungsten field emission pattern has a triangular symmetry, which is due to the way the electrons interfere with each other as they leave the various tungsten crystal planes. An example is shown for comparison in figure 4.2.2.2.

### 4.3 STABILITY

Stability is a contentious subject because, whilst it is possible to make qualitative statements about the stability of electron sources, there is ambiguity when making quantitative statements. There have been numerous values quoted for stability for various electron sources [2-4], but in all of these publications the authors never actually define what they mean by stability. It is puzzling to see how the true merits of various electron sources can be compared when authors arbitrarily define the time over which the stability of a source is measured and do not state this when quoting the result. Authors also do not state whether they are measuring the standard deviation, the variance or the peak-to-peak variation in the electron source beam. If one were to take a cynical stance, it appears that from some of the values presented in journals, the

time over which the stability is measured has been deliberately chosen so that the source measured compares favourably to others. It has been confirmed to the author by some of the most senior experts in electron beam analysis that there is no standard definition for stability. This seems bizarre considering that the stability of the source is its most important attribute.

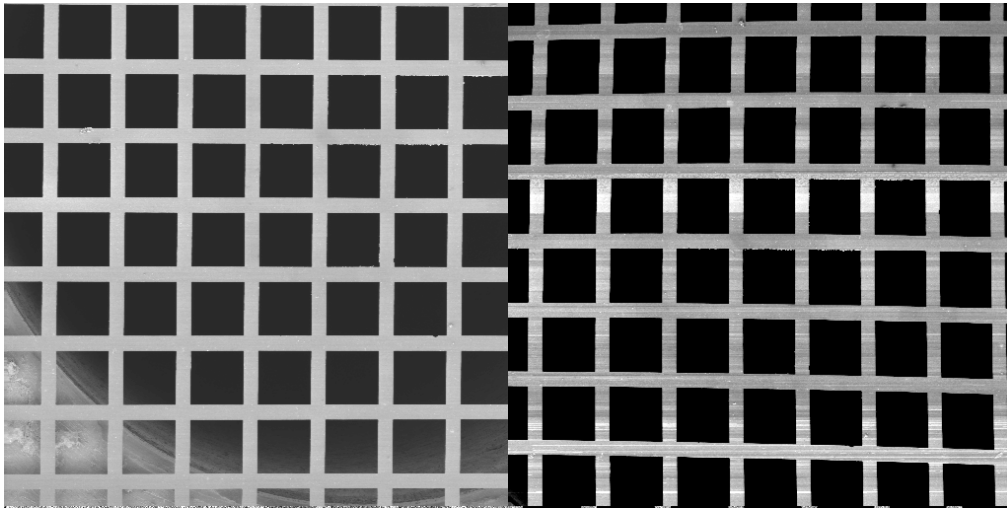


Figure 4.3.1: Two electron micrographs of the same metal grid, *left* with a stable electron source, *right* with an unstable electron source. Whilst the grid appears to be uniform in the left-hand picture, banding appears in the right-hand picture due to a variation in the intensity of the beam.

There are reasons for the lack of a clear definition. There are different time limits over which it is desirable for the current to remain uniform. For instance, it would be inconvenient whilst trying to focus using the TV mode function for the screen to be flickering all the time. A typical SEM session could be anything from 15 minutes to 4 hours or more. A low variation in the beam current would be desirable over this time frame. Also, a high quality image takes about 10-20 seconds to capture, so a high degree of uniformity would be required over this relatively short time-scale in order to capture a high quality image. In figure 4.3.1, for example, two high quality images of the same grid are taken, one with a stable source, one with an unstable source. The unstable source shows banding across the screen. The source scans the same horizontal line a few times, but because the intensity of the beam varies, the bright areas will vary in intensity as the beam moves down the image, causing contrast on a uniform metal grid that does not actually have any contrast.

Finally, returning to TV mode, several images are captured per second as the microscope operator scans across the sample. Therefore, the beam has to remain stable over small fractions of seconds in order to obtain clear images.

These are the various time scales over which the beam needs to be stable. The intensity can be controlled by electronic feedback loops to stabilize the current, but over what time period would they react and under what voltage constraints?

One must also consider the field emission pattern itself. Though the total current may appear to be stable, emission sites continue to switch on and off, their effects often cancelling each other out. The values of stability quoted vary from paper to paper. Some use total current, some use (Faraday) cup current when the two are not the same. The stability of the cup current will depend on the size of the cup, how far it is from the source and the geometry of the system.

The instability data will be presented first, then there will be a discussion of how best to analyse it. Measurements were made at a pressure of  $5 \times 10^{-10}$  mBar or below unless stated otherwise. The tips were also operated at a moderate temperature with a filament current which corresponded to roughly 500 °C. The temperature was determined by plotting filament current against temperature measured by pyrometer for various temperatures above 800 °C. The curve was then extrapolated back to lower temperatures to estimate temperatures for lower filament currents.

### **4.3.1 DETERMINATION OF DRIFT AND INSTABILITY**

To measure stability, it was determined that the best way to measure it would be to use the total current. The total current gives more information about the overall stability of the source. The use of cup current only shows the effect adsorbates have on a particular site. Such information is not necessarily representative of all carbon nanotube sources. The total current may exhibit greater instability than the cup current if instability is due solely to the effect of adsorbates. This is because it is possible for more than one adsorbate to attach to a tip at any one time but they might not necessarily attach to a point that would affect the cup current. The optimum geometry

of the source has yet to be determined, and geometry varies from system to system. Total current is not affected by changing geometries and is a more useful form of comparison with carbon nanotube stabilities measured using other methods by other people [2].

Figure 4.3.1.1 shows the variation in total current,  $I_{tot}$ , with time, of an FEI tip in the second week of field emission. Readings were taken every 20 seconds for a week. The extraction voltage was kept constant for four different values and over varying time frames. It shows a more stable source than the first week of data. It also shows greater stability at lower extraction voltages and total currents.

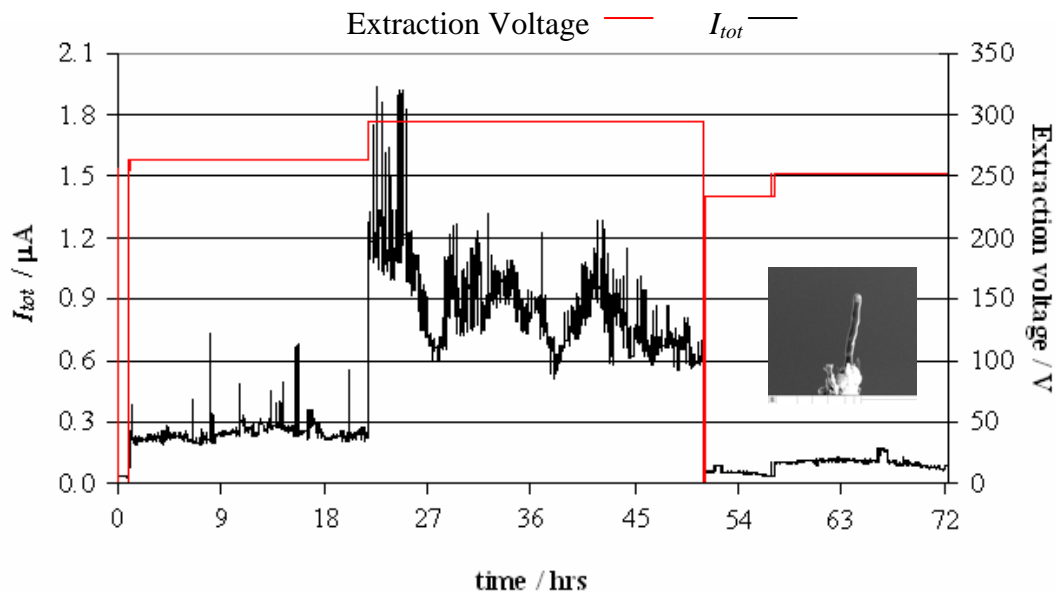


Figure 4.3.1.1: Field emission measurements in the second week. Qualitatively, the source appears to have stabilized further with current varying less than in the first week. Four different extraction voltages were tested, with the higher voltages causing greater instability.

It can clearly be seen in figure 4.3.1.1 that the drift varies randomly and depends on extraction voltage. This is at odds with the data presented by de Jonge (as described in chapter 1) where he suggests that the total current only increases through drift. Figure 4.3.1.2 shows how the current from the tip in figure 4.3.1.1 varies at the lowest extraction voltage. It shows that field emission from the CNT exhibits a step-like structure, where the current jumps to and from various fixed values. This effect is

typical of all the CNTs tested and is a result of adsorbates attaching to and detaching from the tip. This behaviour can be corrected for and is of little interest in terms of stability measurements. What is of interest is how the current varies *within* each step.

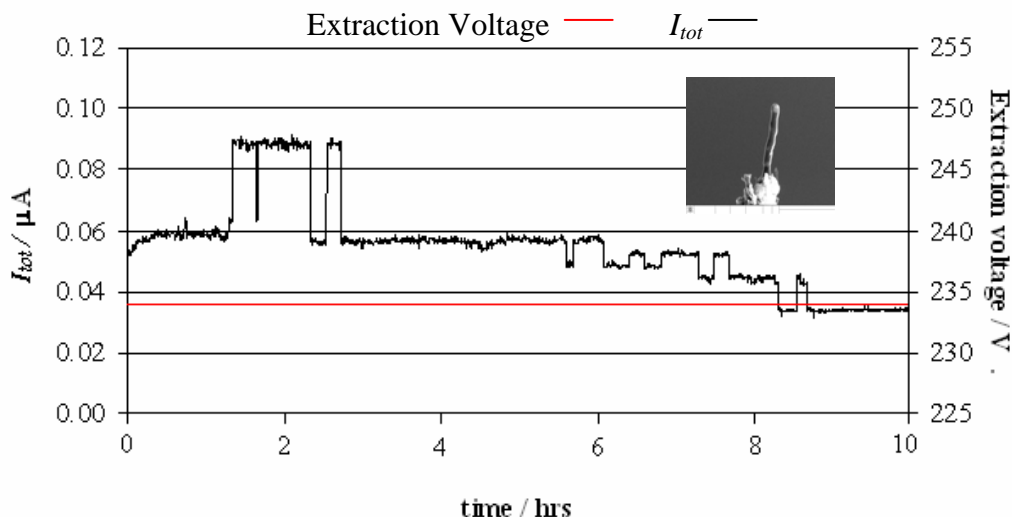


Figure 4.3.1.2: Variation of total current at a constant extraction voltage of 234 V. Emission takes the form of a step-like structure, where current flips between constant currents of different value.

Table 4.3.1.3: The drift of a CNT in its second week of field emission testing at four different extraction voltages.

Extraction voltage / V	Average total Current / $\mu\text{A}$	Drift %		Average drift %
		1	2	
234	0.056	7.3	7.4	7.4
252	0.110	7.0	7.8	7.4
263	0.209	5.7	7.3	6.5
295	0.676	17.6	18.8	18.2

A commonly used definition of stability is to measure how the current varies over the course of one hour. The maximum current and the minimum current is recorded, the latter subtracted from the former and expressed as a percentage of the average current over that hour. This is defined as *drift*. Since the geometry of each CNT is slightly

different, instead of expressing the drift in terms of the extraction voltage, it is better to express it in terms of the average current so that CNTs can be compared to each other. Table 4.3.1.3 summarizes the behaviour of the CNT used in figures 4.3.1.1 and 4.3.1.2 during the second week of data collection. Two drift measurements were made at each extraction voltage.

It is clear from table 4.3.1.3 that at higher total currents, instability increases. When considering the actual numbers involved, the drift is equal to that quoted by others for tungsten cold field emitters (~6%). But is a peak-to-peak measurement a fair representation of the stability? All field emitters are susceptible to current spikes. Sometimes, a large molecule can attach itself to the tip, remain for a few seconds and then remove itself again. The emission can be largely stable the rest of the time. A fairer representation of stability should minimise the influence of these events.

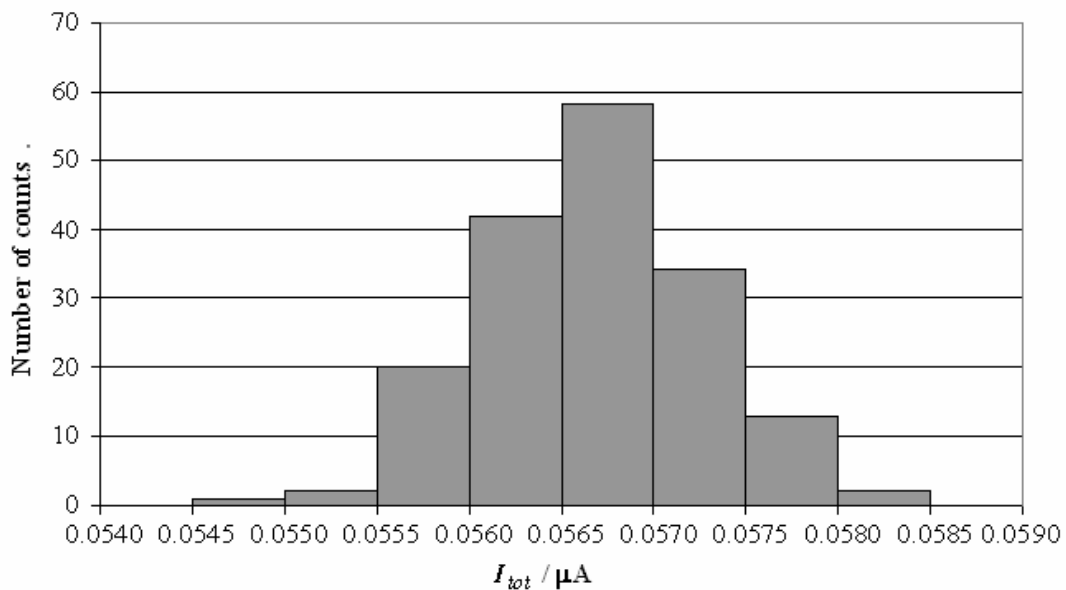


Figure 4.3.1.4: Distribution of the total current,  $I_{tot}$ , over the course of an hour. Most of the current readings are centred on the mean of 0.0566  $\mu\text{A}$ . The distribution appears to be roughly Gaussian in shape.

Figure 4.3.1.4 indicates that the variation in current roughly follows a Gaussian distribution. This indicates that a simple standard deviation treatment of the result would give a more fair representation of the instability of the source.

Theory states that for a Gaussian distribution 63% of all data is within one standard deviation of the mean. Assuming current within each step follows such a distribution, the *instability is defined as* the standard deviation of a total current measured over one hour at twenty second intervals. This definition deliberately uses instability rather than *stability*, which is counter-intuitive; if stability increases, the number should go up rather than down). The same data in table 4.3.1.3 is reworked in table 4.3.1.5.

Extraction voltage / V	Average total Current / $\mu\text{A}$	Instability %		Average instability %
		1	2	
234	0.056	1.1	1.2	1.2
252	0.110	1.2	1.4	1.3
263	0.209	1.3	1.3	1.3
295	0.676	2.8	3.9	3.4

Table 4.3.1.5: The instability of a CNT in its second week of field emission testing at four different extraction voltages.

The data in table I still show that for higher currents the instability of the carbon nanotube decreases. It also shows the stability to vary little at lower voltages.

When describing stability, should both the drift and the instability be quoted to describe the quality of the source? The next section will discuss this in more detail.

### 4.3.2 VARIATION OF INSTABILITY WITH TIME

The data taken in the previous section was for a tip in its second week of data. It is important to determine how the instability of the tip varies with time, and therefore how long it takes for the instability to get to a level where treatment of the tip is required.

Figure 4.3.2.1 shows how both the stability and the drift of the tip in the previous section varied at random times during its lifetime. The data was not corrected for step changes, which explains why the values on the graphs are much higher than those quoted in tables 4.3.1.3 and 4.3.1.5. It is, however, useful to see this information, as it indicates how many step changes occur and how big they are, because the information can be used to work out how to optimise a feedback loop to minimise step changes. Note how the profile of both stability and drift follow each other very closely.

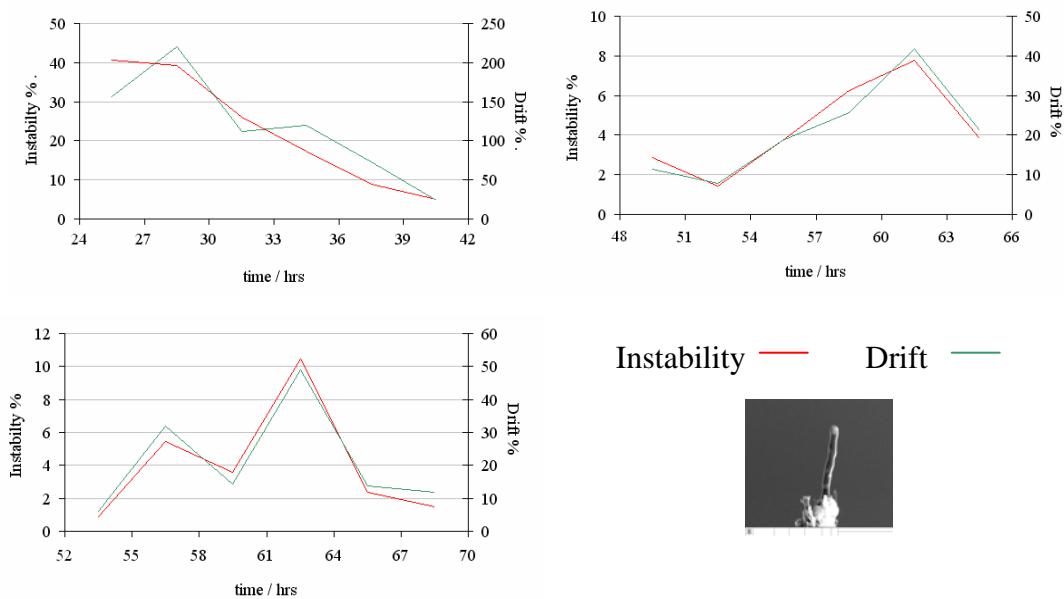


Figure 4.3.2.1: Plots of instability and drift with time at various points during the lifetime of a CNT tip. The data top left were taken in the first week, top right in the second week, bottom left in the third week. This data has not been corrected for step changes in current. Note how the profiles of instability and drift follow each other very closely.

Figure 4.3.2.2 shows the same data in figure 4.3.2.1 but modified for step changes, so now only working out the change in total current within a step. Again, drift and instability follow each other very closely.

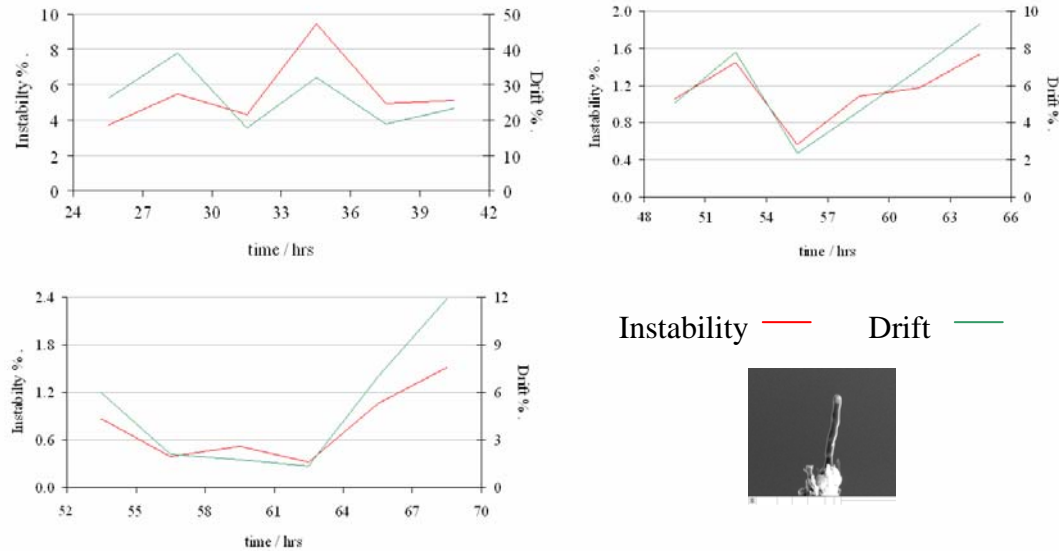


Figure 4.3.2.2: Plots of instability and drift with time using the same data as in figure 4.3.2.1 but corrected for current jumps. The data top left were taken in the first week, top right in the second week, bottom left in the third week of emission. Note how the profiles of instability and drift still follow each other very closely and also note the very low values for both drift and instability in the third week.

Given both uncorrected and corrected field emission data give similar instability and drift profiles, it emphasises the arbitrary nature with which stability is quoted in literature. The mechanism that causes the instability is such that the way in which one analyses the data does not give a significantly different interpretation of stability. Only the absolute values are different. An industrial standard needs to be set so that the various merits of electron sources can be compared properly. It seems that as a rule of thumb (and as illustrated by figures 4.3.2.1 and 4.3.2.2), instability tends to be about a fifth of the value of drift.

In the third week, the tip exhibited remarkable stability at low total currents as illustrated in figure 4.3.2.2 and as can be seen in table 4.3.2.3. This can be explained by a self-cleaning process. By the third week, a significant proportion of the gas adsorbed during the fabrication process will have now desorbed.

Table 4.3.2.3: Typical values of the instability and drift of a CNT over a three week period.

Week number	Extraction voltage / V	Average total current / $\mu\text{A}$	Average instability %	Average drift %
1	252	0.106	2.0	8.7
2	252	0.110	1.3	7.4
3	246	0.125	0.6	3.1

Note how the average total current slightly increases even though the extraction voltage has decreased over time. The tip was not moved, the geometry was not changed and the pressure in the system remained constant. This seems to be an anomaly peculiar to CNTs. Figure 4.3.2.4 illustrates how a CNT, whose characteristics were measured at Philips Research Laboratories, Eindhoven, The Netherlands, emits when the total emission current is held to be within 10% of a preset value, in this case 100 nA. It shows the CNT's behaviour during its first 7 hours of emission, hence the noisy behaviour. Note how the extraction voltage falls from 800 V to as low as 460 V over the course of the 7 hours. The extraction voltage would eventually fall to 350 V.

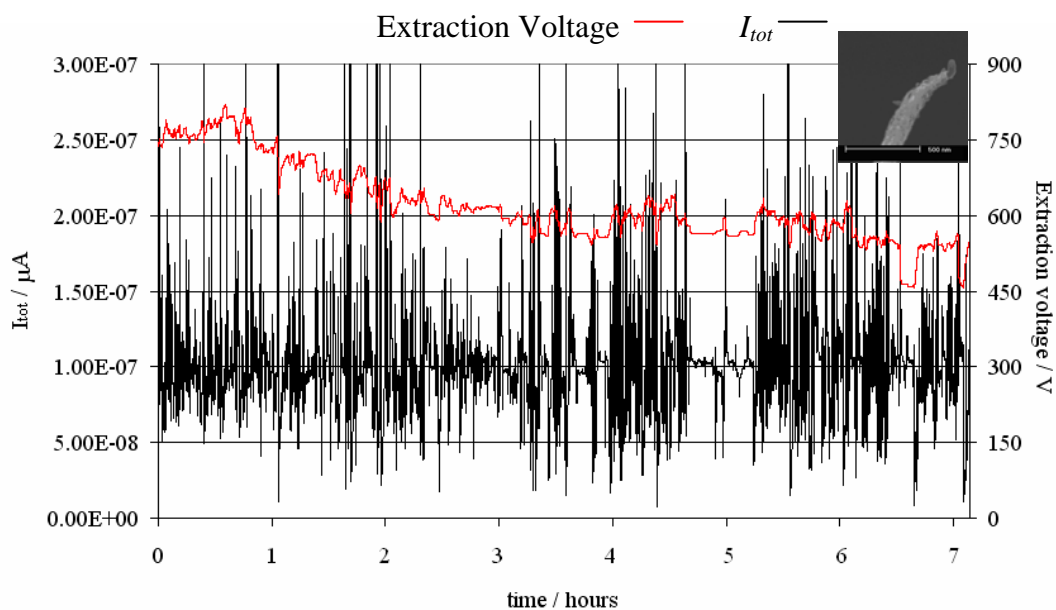


Figure 4.3.2.4: Variation of extraction voltage for (roughly) constant total current,  $I_{tot}$ , over the first seven hours of emission.

Because everything in the system is fixed, one can only assume that either the shape of the cap is changing, or that the workfunction is changing. Yet, we know that the shape of the CNT does not change in field emission as can be seen in figure 4.3.2.5.

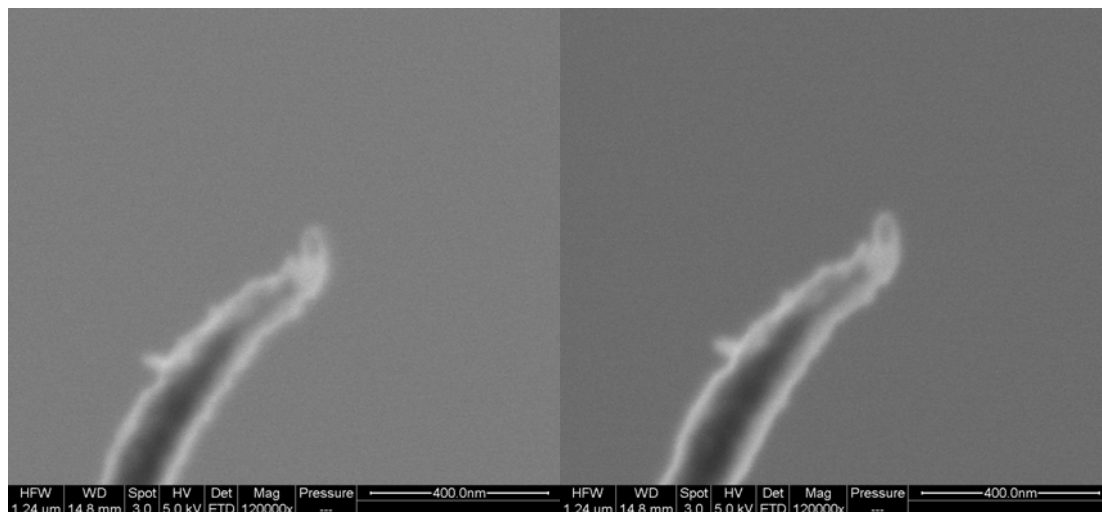


Figure 4.3.2.5: The source used in figure 4.3.2.4 before (left) and after (right) field emission experiments. No change is observed in the tip structure.

Therefore we must conclude that the workfunction is continuously altering during the cleaning process. This could be due to adsorbants desorbing. This assumes that the adsorbed species increase the workfunction because the initial extraction voltages are higher. Alternatively, the chemical structure of the CNT could be changing. It could be that the electrical resistance of the tip is continually and gradually reducing due to the atoms rearranging throughout the CNT, or through additional and more conductive bonds forming through the application of heating, reducing the resistance at the interface between the CNT and the tungsten tip. The nature of the bond at the interface is uncertain and requires further investigation. It would also be very difficult to confirm whether or not the chemical structure of the CNT is changing because the signal from a Raman spectrum, for instance, would not be strong enough to detect.

After week three it was found that the characteristics of the tips did not significantly improve, though it was found over time that instability would increase slightly. This is probably due to dirt in the system attaching to the tip and altering the field emission by altering the workfunction slightly. There are two methods to combat this; both operate on the same principle and both effectively employ “flashing” the tip, or the

rapid heating of tip, which is a common treatment for reducing instability and drift in cold field emitters.

For instance, applying heat at 1000 °C for 10 mins in the first hour of tip FEI01's lifetime resulted in a decrease in instability from 6% to 3% and a decrease in drift from 27% to 18%. Heating was carried out by passing a current of approximately 3.2 A through the heating filament of the tungsten wire bridging the two feedthroughs and with the temperature monitored by a pyrometer. If the tip were made to a standard model, a pyrometer would not be required and a pre-determined current could be passed through the heating filament to flash the CNT tip.

The other method used to increase stability was to increase the total current by a factor of 10, hold it there for an hour and to then return to the previous total current preset. For the same tip and for a similar total current but in the following week, as a result of this treatment, the instability decreased from 4.6% to 1.4% and the drift from 16% to 5%.

Both methods involve heating the CNT which probably causes adsorbates accumulated on the tip to desorb back into vacuum.

#### **4.4 CNT TIP LIFETIME**

Without heat treatment, the tip degrades. Figure 4.4.1 shows how instability for a tip with constant extraction voltage varies with time. The initial measurement shows high instability for the first day which is in keeping with the characteristics of other CNT tips, falling away to 1% instability after five days. At 11 days the instability increases to around 8% where it stays for a month. Beyond a month the instability increases until after 6 weeks the instability becomes so large that the tip disintegrates. Figure 4.4.2 compares the instability of the tip on the eighth day with that of the fortieth day. It is clear that the emission is significantly more unstable on the fortieth day.

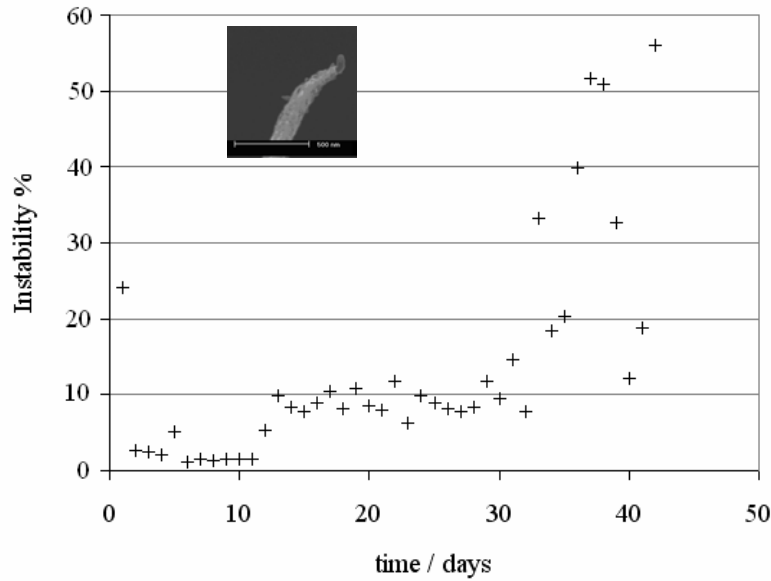


Figure 4.4.1: The variation of average instability over the course of a day with time. The total current was set at 100 nA to begin with, but generally increased with time. The tip broke after 42 days.

Because of the relatively short duration of the PhD, it was not possible to do long lifetime tests on any CNT tips. This is the longest any CNT that has been measured in this work, because all CNTs were tested to destruction. It is important to determine the various parameters which cause the CNTs to fail if the source is ever to reach market. Though De Jonge et al recorded field emission from a CNT for sixteen months, this was with the use of a feedback loop together with regular flashing. The feedback control keeps the emission within total current limits, adjusting extraction voltage accordingly. This prevents the current from exponentially increasing to a point that self-heating vaporizes the CNT. Flashing reduces instability and drift which also acts to postpone thermal runaway from occurring.

It should also be noted that the way in which the tips are flashed could also affect the tip's lifetime. Variations in temperature and duration can effect the stability of the emission after flashing.

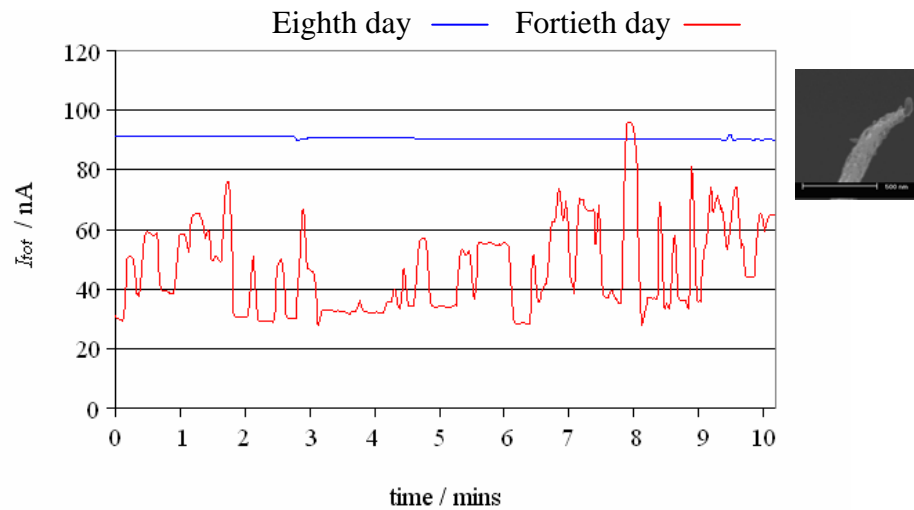


Figure 4.4.2: The total current,  $I_{tot}$ , plotted over a ten minute period on the eighth day in blue and the fortieth day in red. It is clear that the instability is much higher on the fortieth day which is probably due to the lack of flashing.

#### 4.5 VARIATION OF INSTABILITY WITH PRESSURE

As stated previously, field emission measurements were made at  $5 \times 10^{-10}$  mBar or below. Measurements were taken to see how the instability varies with pressure. Figure 4.5.1 compares typical instability and drift of a tip at three operating pressures for extraction voltages giving total currents of approximately 100 nA over similar timeframes.

There are few data points because the data takes so long to collect. However, it is clear that there is a general trend towards greater instability at higher operating pressures. This is summarized in figure 4.5.2 below, where the average drifts and instabilities in the above graphs are plotted as a function of pressure. Operating at pressures in the mid  $10^{-9}$  mBar range and below seems to produce instability at an acceptable level. However, at  $10^{-8}$  mBar, instability increases hugely. CNTs should not be operated at these pressures or worse.

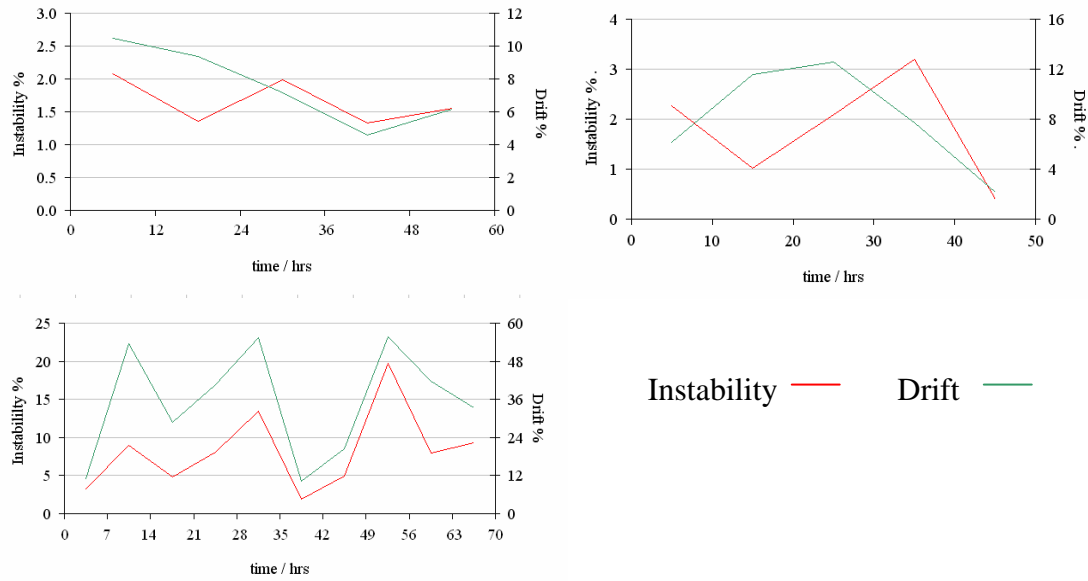


Figure 4.5.1: The variation of instability and drift with time at different pressures. Data in the top left-hand graph were taken at a pressure of  $5 \times 10^{-10}$  mBar, data in the top right-hand graph were taken at  $3 \times 10^{-9}$  mBar, and data in the bottom left-hand graph were taken at  $1 \times 10^{-8}$  mBar. There is a significant difference in magnitudes between the two graphs, and a general trend to greater instability the higher the pressure.

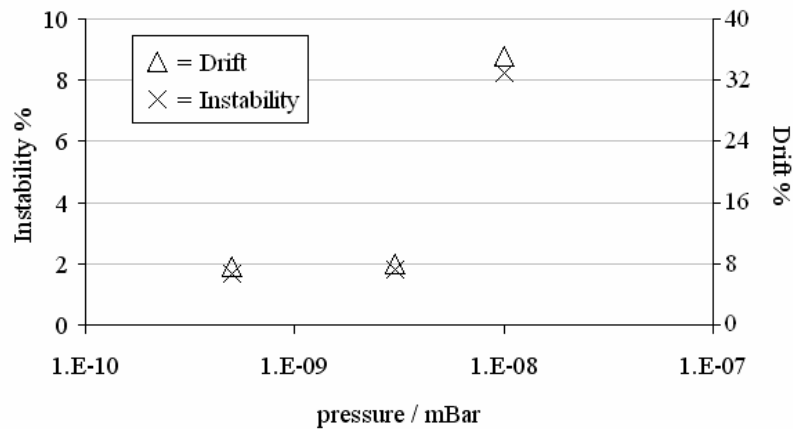


Figure 4.5.2: Averaged instability and drift as a function of pressure. There is a huge increase in instability at or before  $1 \times 10^{-8}$  mBar.

#### 4.6 WORKFUNCTION OF CNT ELECTRON SOURCES

Once the CNT has settled down and is giving stable field emission, it is straightforward to determine the workfunction by finding the I-V characteristics and plotting a Fowler-Nordheim curve ( $1/V$  against  $\ln[I/V^2]$ ). Figure 4.6 shows data taken from two stable, emitting CNTs.

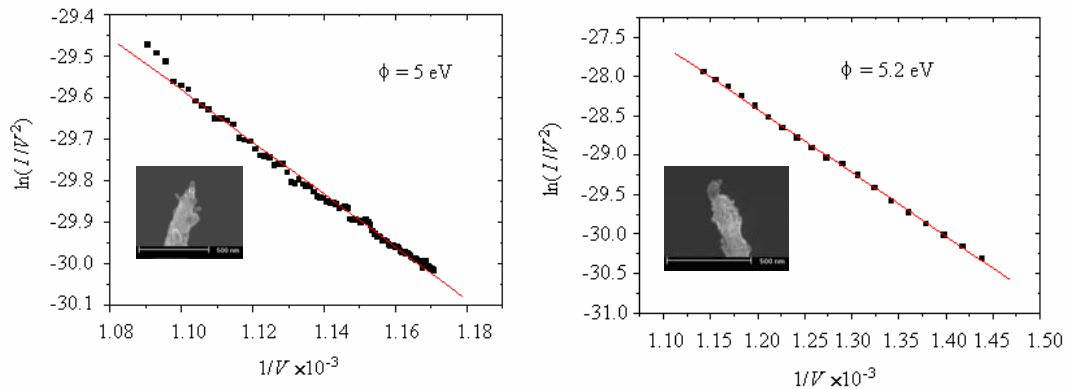


Figure 4.6: Two Fowler-Nordheim curves for separate CNTs. Both produce workfunctions of approximately 5 eV, which is approximately the workfunction obtained for graphene and other nanotubes mentioned elsewhere in the literature.

Given the plot is a straight line it is safe to conclude that this is a Fowler-Nordheim-based field emission process. Emission due to thermal excitation would show deviation from this line. Given the Fowler-Nordheim equation and the various parameters within it in the rig, it was possible to determine the workfunction of the CNTs to be 5.0 and 5.2 eV respectively. This is approximately equal to values obtained elsewhere in literature, but it is also approximately equal to the workfunction of tungsten. Therefore, workfunctions do not prove that the emission is coming from the CNT, it merely proves that we have field emission. However, the field emission pattern indicates that field emission is coming from a CNT.

#### 4.7 ENERGY SPREAD MEASUREMENTS

A low energy spread is one of the key reasons CNTs have been earmarked as potential electron sources. It was not possible to measure energy spread with the FEI

experimental setup. The ability to carry out energy spread measurements relies on two parameters, how stable the source is and the degree to which the CNT is aligned. This is because the beam is accelerated and decelerated whilst passing through a series of small apertures in plates at different voltages; a slight deviation from the optical axis prevents the beam from passing through all the holes. For an unstable source, intensities go up and down, meaning that signals will be irregular when one scans through the various beam energies. The FEI method for attaching single pieces of tungsten wires with CNTs already grown upon them to the heating filament outlined earlier results in poor alignment with the column axis. Furthermore, there was little room to manoeuvre the CNT source once it was in the measuring system. Trial and error was the only way we could have achieved measurement of energy spread by this method. After many attempts, this avenue was abandoned.

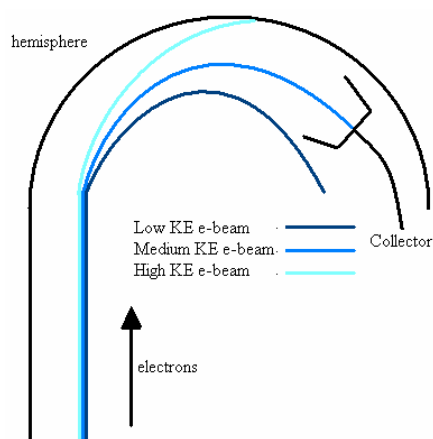


Figure 4.7.1: Schematic representation of the kinetic energy spread measurement apparatus. The electron beam enters from the bottom. Fast electrons crash into the metal hemisphere, slow electrons are deflected too much and miss the collector, electrons are only deflected into the cup if they are travelling at the speed required which is dependent on the field applied to the hemisphere.

Consequently, energy spread measurements were made at Philips Research Laboratories, Eindhoven following the growth of CNTs on specially designed, pre-aligned hairpins. The equipment in Eindhoven allowed for manoeuvring once the CNT source is placed within the testing rig. The equipment at Eindhoven differed slightly from the equipment used at FEI. The electron beam passes into a hemisphere,

whose voltage can be varied to deflect the beam by differing amounts. A collector is placed three quarters of the way round the hemisphere. Electrons of too little energy will be deflected too much by the electric field whilst electrons of too much energy will not be deflected enough to be collected and crash into the hemisphere before reaching the collector. By varying the voltage on the hemisphere, one can scan through the various beam energies and measure the amount of electrons deflected into the cup to obtain a kinetic energy distribution in the beam (schematic shown in figure 4.7.1).

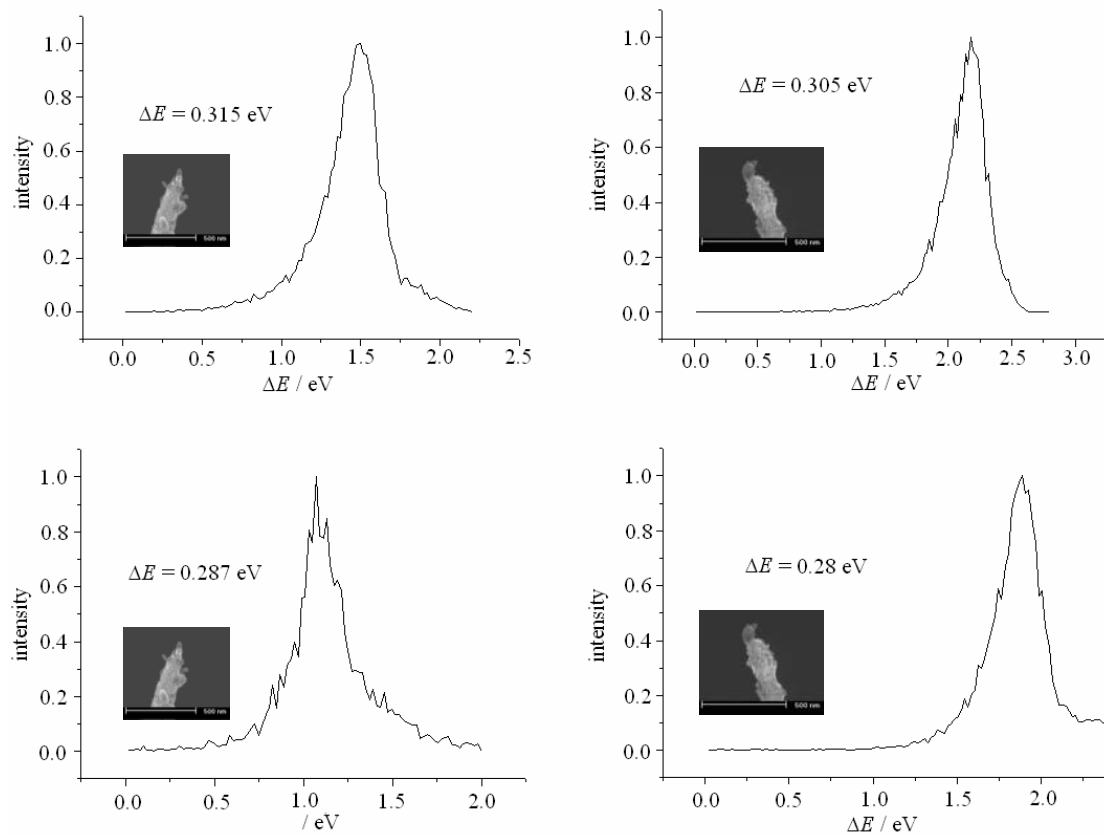


Figure 4.7.2: Some of the best energy spread measurements achieved by CNTs grown on tungsten tips at Cambridge. Top-left was achieved at  $I_{tot} = 104$  nA,  $T = 500$  °C. Top-right was achieved at  $I_{tot} = 40$  nA,  $T = 500$  °C. Bottom-left was achieved at  $I_{tot} = 100$  nA,  $T = 500$  °C. Bottom-right was achieved at  $I_{tot} = 80$  nA,  $T = 500$  °C.

Measurements were made on three CNTs. None produced the low energy spreads of 0.20 eV mentioned elsewhere [2,3], though it should be emphasised that the lowest energy spreads were obtained at  $\sim 1$  nA total current, a current far too small to

determine kinetic energy spreads with our set-up. Some of the best energy spread measurements, defined as the full-width, half-maximum of the intensity are shown in figure 4.7.2.

Another explanation for not achieving the low kinetic energy spreads observed by de Jonge et al [2] is that despite the thermal annealing treatment, the CNTs still are not of the same quality as those grown by arc discharge. Extra resistance within the CNT could be the cause of a greater energy spread. That said (and as can be seen in figure 4.7.3), the kinetic energy spreads fit onto de Jonge's curve of total current against energy spread.

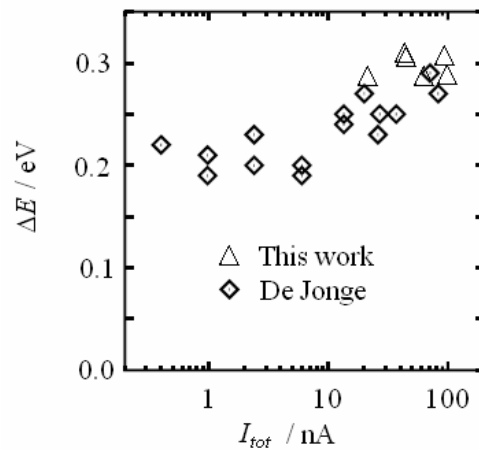


Figure 4.7.3: Graph comparing the total current,  $I_{tot}$ , against the kinetic energy spread,  $\Delta E$  for De Jonge's tips [2] and this work. CNTs measured at 100 nA exhibit similar kinetic energy spreads to that measured for CNTs during this project.

Although operated at higher total currents than those used by De Jonge et al [2], the trend exhibited in  $\Delta E$  is replicated for CNTs grown as part of this PhD. It is questionable whether CNTs would ever be used in the 1 nA regime. CNTs are bright, but not 100 times brighter than Schottky sources and certainly not 100 times brighter than tungsten cold field emitters. To image a sample, one needs a signal. What is the merit of declaring CNTs to have an energy spread of 0.2 eV when you are never going to use them in this regime? One could equally say that the energy spread is 0 eV for 0 total current.

Figure 4.7.4 shows measurements taken at both 500 °C and room temperature. Theory states that at lower temperatures, the kinetic energy spread should go down. In fact, the kinetic energy spread actually increases because the instability of the source at room temperature (due to adsorbates not being driven off by heating the tip) causes electrons to be emitted at slightly different speeds. This again shows that CNT electron sources should be heated to optimise field emission parameters.

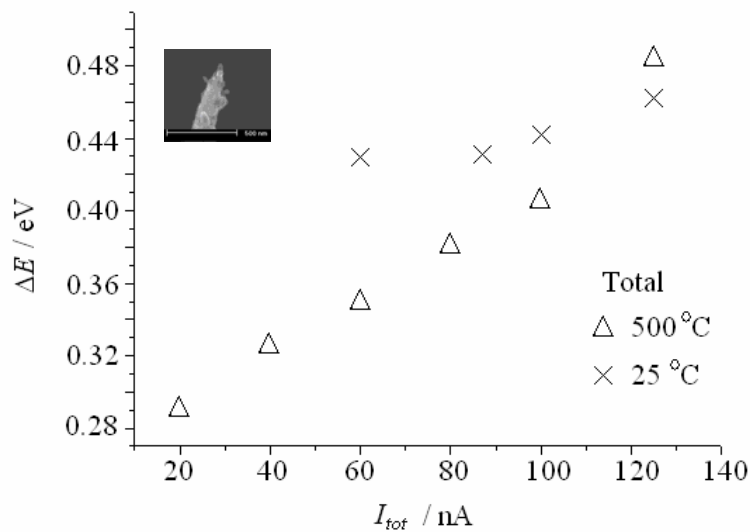


Figure 4.7.4: Graph showing the relationship between the total current,  $I_{tot}$ , and the kinetic energy spread,  $\Delta E$ . This graph shows that contrary to theory, the kinetic energy spread increases at lower temperatures and at total currents less than 100 nA.

#### 4.8 BRIGHTNESS DETERMINATION

Another key factor in the use of CNTs as electron sources is that they have been measured to be significantly brighter than other emitters so far. This is connected to their comparatively small size. It was not possible to measure brightness at Philips Research Laboratories due to time constraints. This would have been the ideal machine to use, since it was the same machine used for De Jonge et al's experiments [2]. However, it was possible to get an approximate value for brightness from measurements made at FEI.

Little mention has been made so far of cup current, which is the amount of current collected in a Faraday cup positioned in the centre of the phosphor screen. The Faraday cup has a finite size (in this case 250  $\mu\text{m}$ ). Given the fixed geometry of the system it is possible to translate the measured cup current into reduced angular current density,  $I'_r$ , which is proportional to reduced brightness,  $B_r$ , (which is also a function of virtual source size  $r_v$ ) as reiterated in equation 4.8.

$$B_r = \frac{dI}{d\Omega} \frac{1}{\pi r_v^2} \frac{1}{U} = \frac{I'_r}{\pi r_v^2} \quad \text{Equation 4.8}$$

where  $I$  is the cup current,  $\Omega$  the solid angle of the Faraday cup and  $U$ , the extraction voltage.

Schottky sources have been measured extensively in the same system. If one assumes that the virtual source size of the CNT is equal to that of a Schottky emitter (it is in fact almost certainly smaller), it will put a minimum value for the brightness upon the CNT source, compared to a standard Schottky source.

Unlike a Schottky source, the CNT source has a series of bright patches (as discussed earlier in section 4.2.1). This means that to get the maximum current, one needs to deflect the beam so that one of the bright patches hits the Faraday cup. In the FEI setup, this was done by magnets. It is possible that in so doing, the beam was slightly attenuated. However, it is not believed that the effect will be significant.

Figure 4.8 shows the field emission from a typical CNT in its third week of emission and plots the reduced angular intensity against time with extraction voltage. It is clear that at higher extraction voltages, the reduced angular intensity reaches 0.4  $\mu\text{A}/\text{srV}$ . With the same system geometry, the maximum obtainable reduced angular intensity has been 0.15  $\mu\text{A}/\text{srV}$  with a Schottky source. This is a threefold increase.

Although this is an approximation, it indicates that the brightness of the CNT is of the order of  $2 \times 10^9 \text{ A}/\text{cm}^2\text{sr}$ , which is even higher than the tungsten cold field emitter. Confirmation of this, together with the source size can only be realistically achieved

by placing the source in a microscope column. This will be covered in the next chapter.

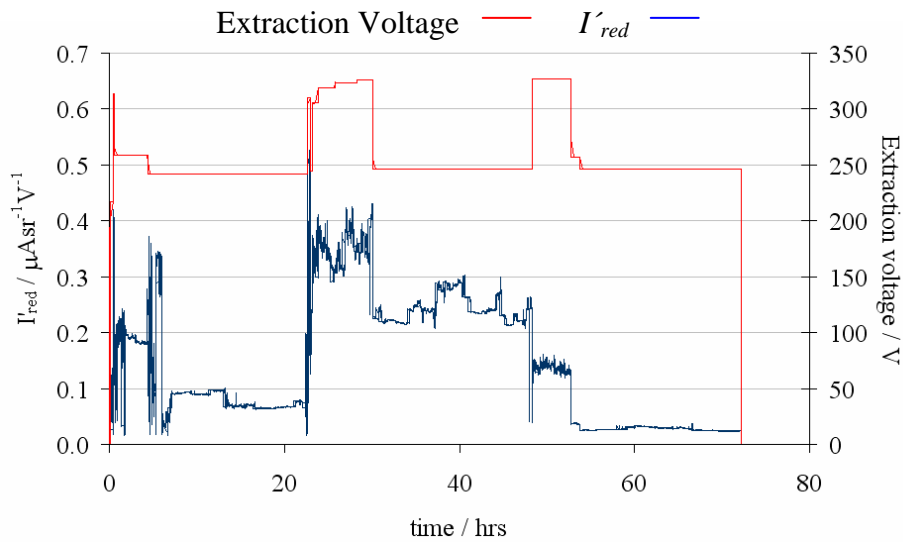


Figure 4.8: Reduced angular intensity,  $I'_{red}$ , and extraction voltage against time. The maximum sustained reduced angular intensity is 0.4  $\mu\text{A/srV}$ .

#### 4.9 SUMMARY

Field emission experiments indicate that the properties of the CNT, whilst excellent, have been exaggerated somewhat. Stability is not significantly better than a cold field emitter though it can be stable over the course of an hour. This work has also defined new ways of quantifying stability with new definitions for *drift* and *instability*. Currently, CNT lifetimes based on results here have not exceeded 6 weeks, but this is a result of driving the CNTs to destruction. Lifetime tests will need to be carried out to determine a typical lifetime for a CNT source. The kinetic energy spread of electrons in the beam was found to be higher than the lowest values quoted by de Jonge et al [2] but only because the measurements they made were typically at unrealistically low total currents. Initial brightness measurements indicate that the CNT is at least half an order of magnitude brighter than the commonly used Schottky emitter.

This data comes from the most extensive work carried out so far into the electron-optical properties of CNTs. It disambiguates stability and is the first proper

comparison between a feasible device and others available on the market. A summary of the key CNT parameters for field emission optimization is given in table 4.9.

Table 4.9: Summary of the key CNT parameters for field emission optimization.

Parameter	Controlled by	Optimum configuration	Best value measured
Brightness	Radius and height of CNT	Minimal diameter, maximal height	$2 \times 10^9$ A/cm <sup>2</sup> sr
Instability (1)	Level of vacuum	Lowest vacuum possible	0.6%
	(2) Degree of flashing	Regular flashing every three days	0.6%
Energy spread	Current and tip temperature	Low current – moderate temperature (500 °C)	0.28 eV

#### 4.10 REFERENCES

- [1] E. Minoux, O. Groening, K.B.K Teo, S.H. Dalal, L. Gangloff, J.-P. Schnell, L. Hudanski, I.Y.Y. Bu, P. Vincent, P. Legagneux, G.A.J. Amaratunga, and W.I. Milne. "Achieving High-Current Carbon Nanotube Emitters", *Nanoletters* 5, 2135 (2005).
- [2] N. de Jonge, N.J. van Druuten: "Field emission from individual multiwalled carbon nanotubes prepared in an electron microscope," *Ultramicroscopy* 95 (2003) 85–91.
- [3] Applied Physics Technologies brochure, 1600 NE Miller St. McMinnville, OR 97128, 2005.
- [4] FEI Company brochure, 5350 NE Dawson Creek Dr. Hillsboro, OR 97124 USA, 2005.